Supplementary Figure S1

Figure S1. The specificity of the primary antibodies was validated.

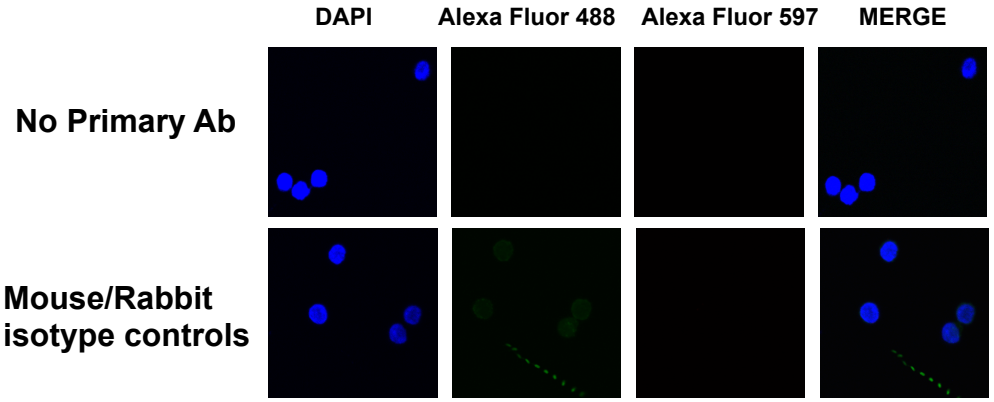

Double immunofluorescent staining was performed in human HCV-infected B cells with no primary antibody or mouse/rabbit isotype controls for primary antibodies. Representative images for Alexa Fluor 488 (green) and Alexa Fluor 597 (red) were captured by confocal immunofluorescence microscopy at ×600 magnification. DAPI, 4′,6-diamidino-2-phenylindole; Merge, merged image of Alex Fluor 488, Alexa Fluor 597, and DAPI.

Supplementary Figure S2

Figure S2. The percentage of NS3 positive cells among CD19 positive cells in human HCV-infected patients was determined by flow cytometry.

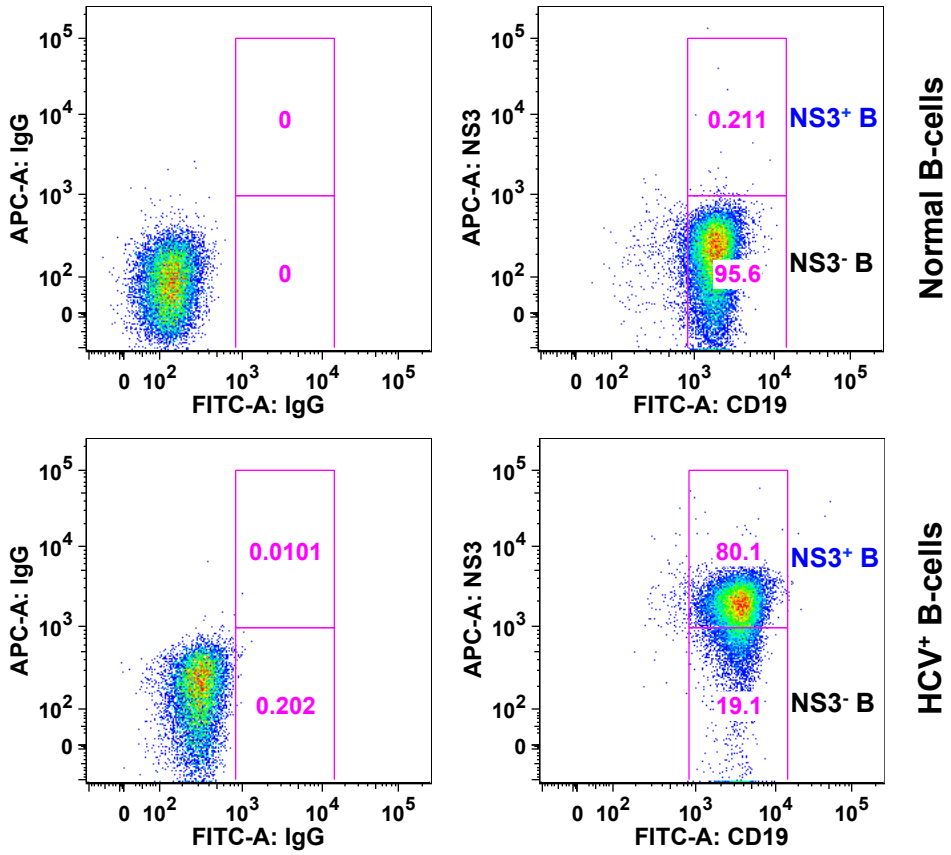

Isolated B-cells from normal and HCV-infected PBMC were stained with FITC anti-human CD19 antibody and Alexa Fluor 647 anti- hepatitis C virus NS3 antibody, as well as appropriate isotype controls. The percentage of NS3 positive cells among CD19 positive cells was analyzed by flow cytometry.

Supplementary Figure S3

Figure S3. Detection of HCV RNA positive and negative strands in normal human primary B-cells and Raji cell line infected in culture with authentic, patient-derived HCV.

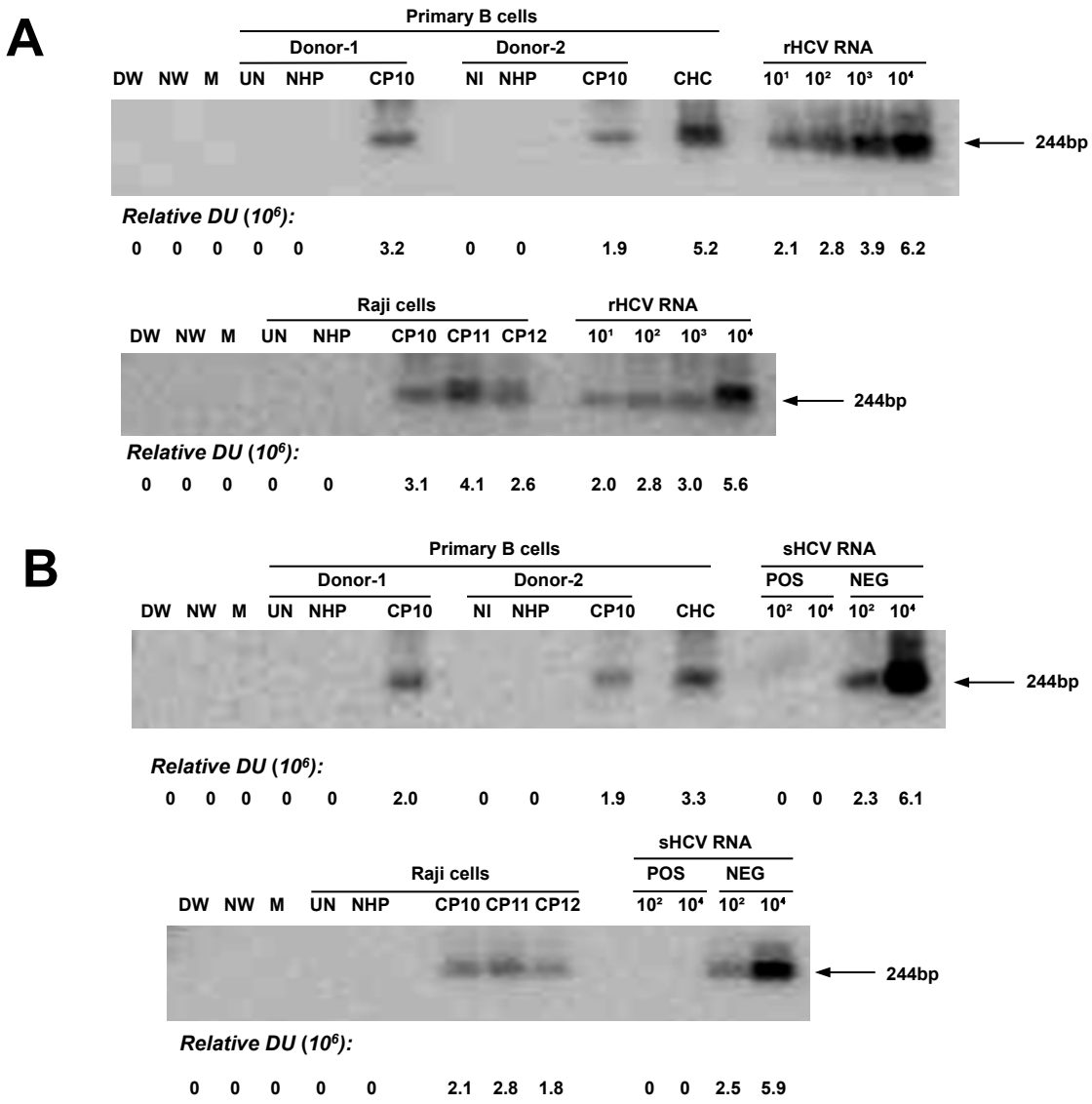

Primary B-cells purified from two donors (donor-1 and donor-2) were exposed to the same copy numbers of HCV from patient 10 (chronic plasma 10, CP10), while Raji cells were exposed to HCV contained in CP10, CP11 and CP12. In all instances, infection was carried out at multiplicity of infection of 1.0. HCV RNA positive and negative strands were identified by RT-PCR/NAH. For positive controls, purified B-cells from a patient with chronic hepatitis C (CHC) and plasma HCV load of 1.6×10^7 vge/ml were used. In all reactions, water amplified in direct (DW) and nested (NW) reactions and a mock (M) extraction served as contamination controls. The positive signals showed the expected 244-bp 5'-UTR sequence-specific fragments. Numbers under the panels represent relative densitometric units (DU) given by hybridization signals. UI, HCV uninfected; NHP, normal human plasma.

A. Identification of HCV RNA positive strand using 1 µg of total RNA. Serial 10-fold dilutions of recombinant HCV 5'-UTR-E2 (rHCV RNA) fragment carrying indicated copy numbers per reaction were included as quantification standards.

B. Detection of HCV RNA negative strand using 3 µg of total RNA. Synthetic HCV RNA positive (POS) strand and negative (NEG) strand at indicated copy numbers per reaction were included as specificity controls.

Supplementary Figure S4

Figure S4. Detection of HCV viral core protein in normal human primary B-cells and Raji cell line infected in culture with authentic, patient-derived HCV.

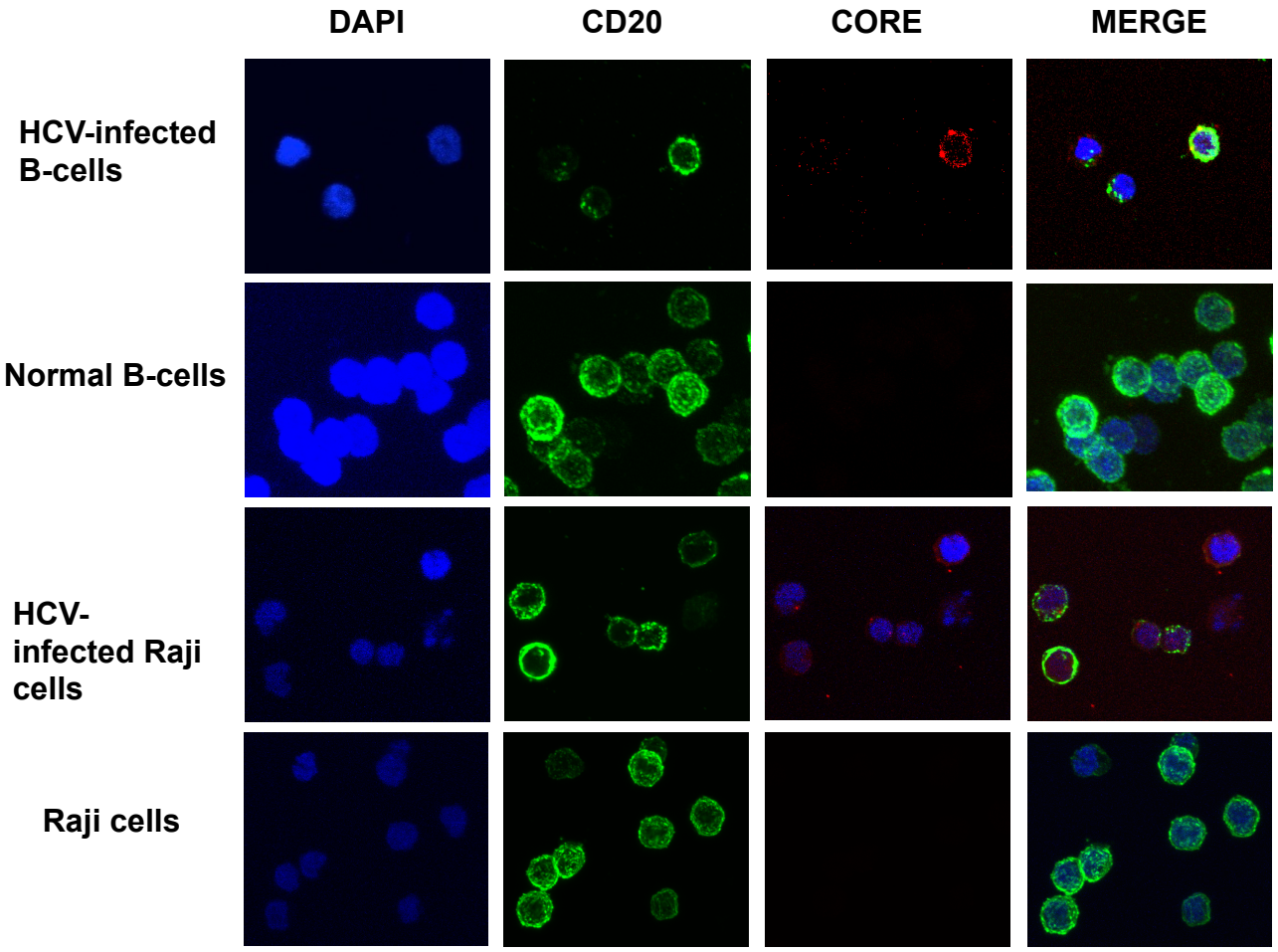

Double immunofluorescent staining was performed in human primary B-cells and Raji cell line infected in culture with authentic, patient-derived HCV as well as their controls. Representative images for HCV core (red) and CD20 (green) staining were captured by confocal immunofluorescence microscopy at ×600 magnification. DAPI, 4′,6-diamidino-2-phenylindole; Merge: merged image of CD20, core, and DAPI.

Supplementary Figure S5

Figure S5. The protease domain of NS3/4A is critical for the interaction between NS3/4A and CHK2 proteins in HeLa and HEK cells.

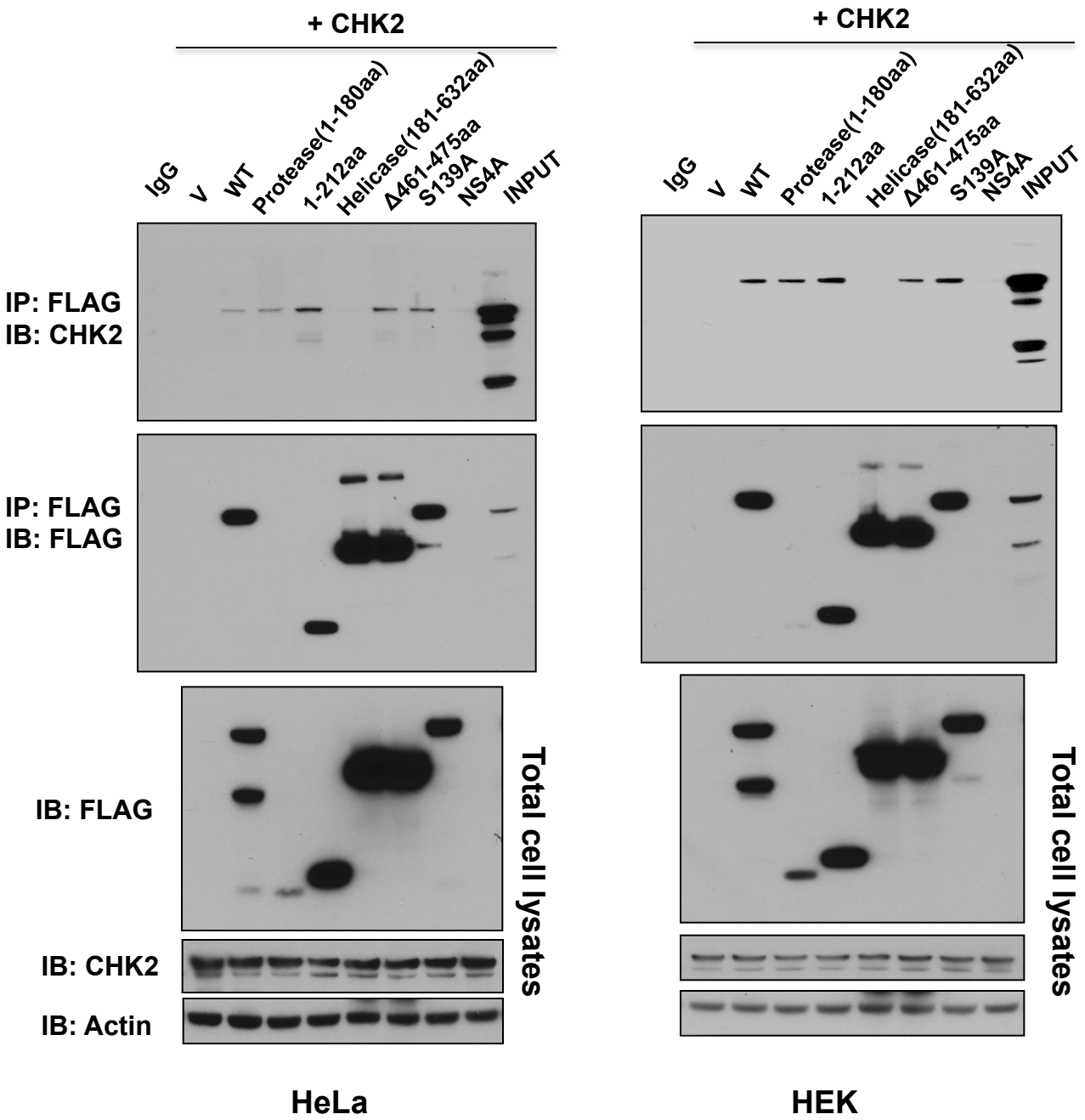

A series of FLAG-tagged NS3 truncation and deletion mutants were co-expressed with CHK2 WT in HeLa and HEK cells. The cell lysates were immunoprecipitated using anti-Flag antibody, followed by immunblotting with CHK2 and Flag.

Supplementary Figure S6

Figure S6. Principal component analysis showing three independent data distributions of each data subset in RIP-Chip system.

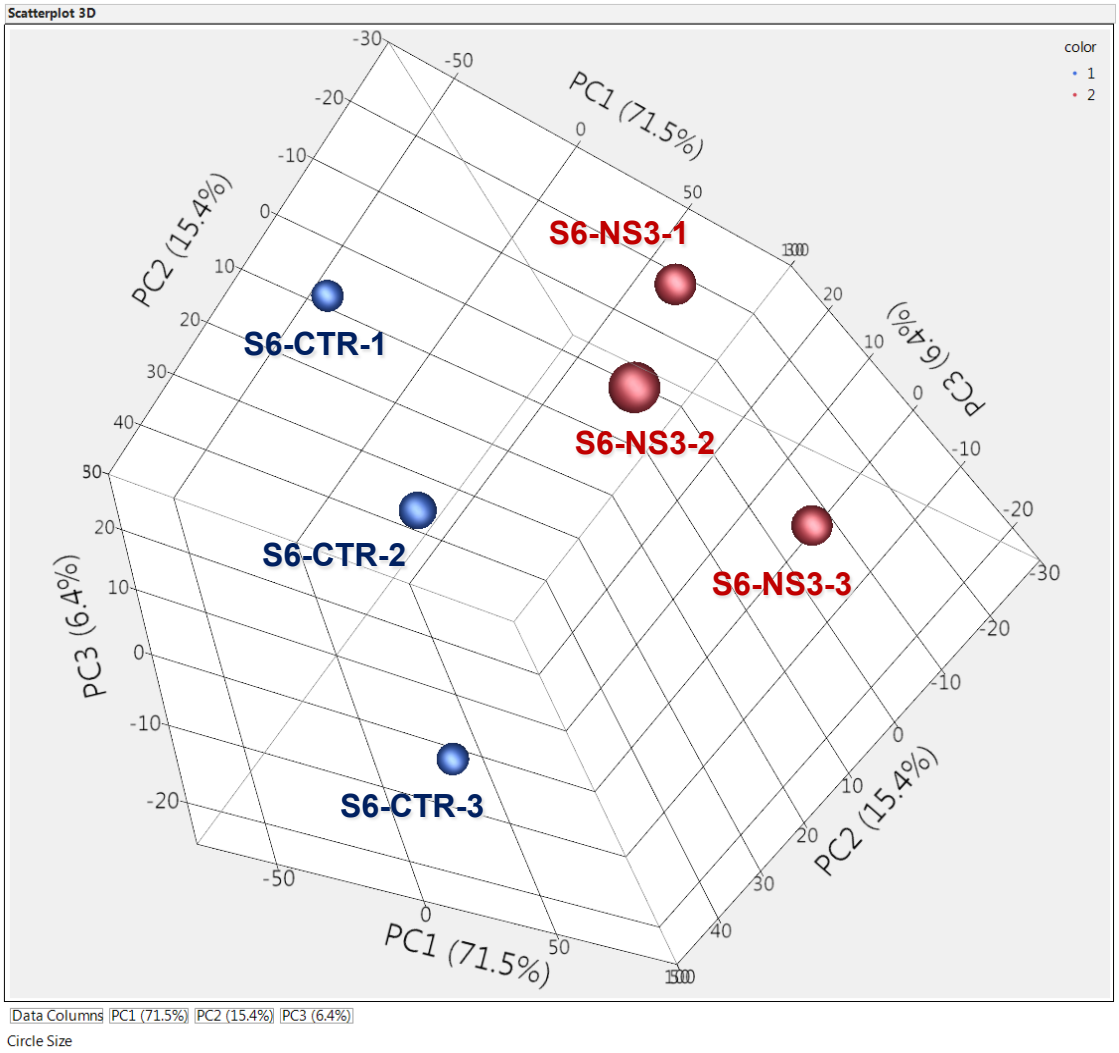

There are three independent data distributions of each data subset that is SUDHL6 vector control (S6-CTR, blue) and SUDHL6-NS3/4A (S6-NS3, red) cells respectively.

Supplementary Figure S7

Figure S7. NS3 mRNA binds to HuR protein.

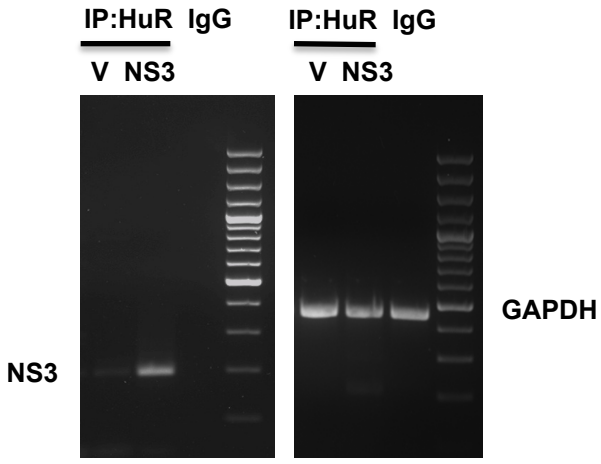

HuR-NS3 mRNA interaction was measured by RNP-IP analysis followed by RT-PCR.

Supplementary Figure S8

Figure S8. Blk and SYK mRNA were stabilized by NS3/4A overexpression in SUDHL6 cells.

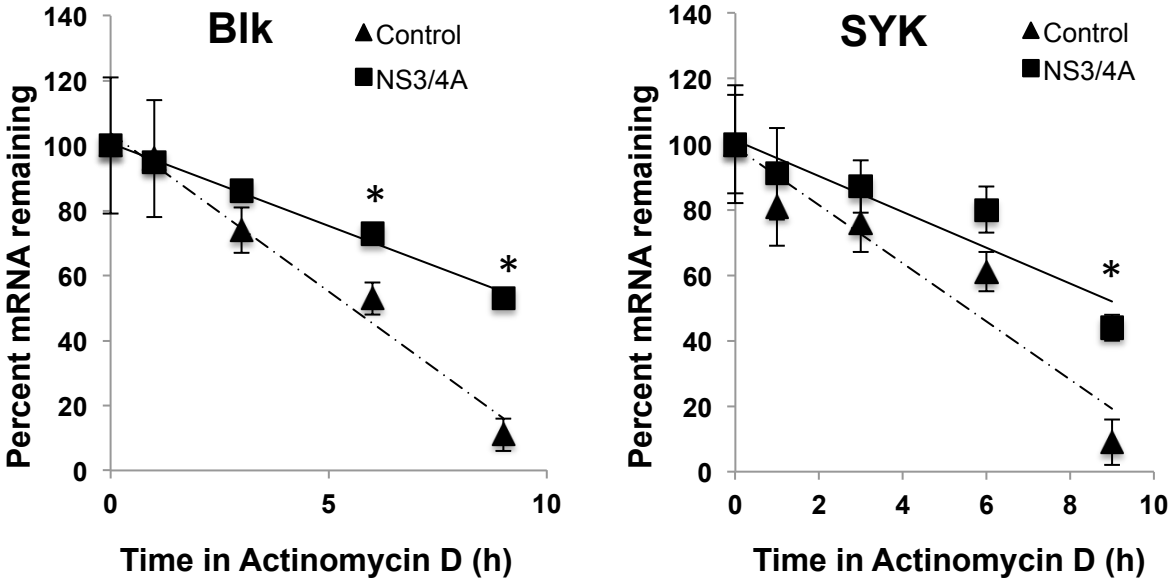

Stabilities of Blk and SYK were measured by incubating SUDHL6 vector control and NS3/4A overexpressing cells with actinomycin D (10μg/ml) for the times indicated. After RNA extraction, the levels of Blk and SYK mRNAs were measured by RT-qPCR analysis and normalized to GAPDH mRNA. Data represent the mean and SD from three independent experiments. *, $p < 0.05$

Supplementary Figure S9

Figure S9. The protein expression of BCR signaling pathway components is up-regulated by NS3/4A overexpression in SUDHL2 cells.

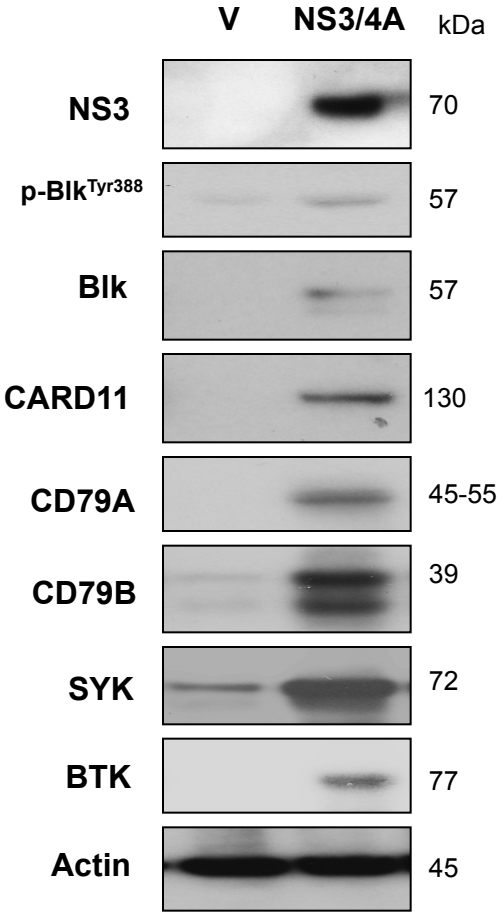

Western blot analysis showing protein expression of selected HuR targets in whole cell lysates of vector control (V) and SUDHL2-NS3/4A cells. Actin was used as a loading control.

Supplementary Figure S10

Figure S10. Global protein synthesis is not changed in SUDHL6-NS3/4A cells versus control cells.

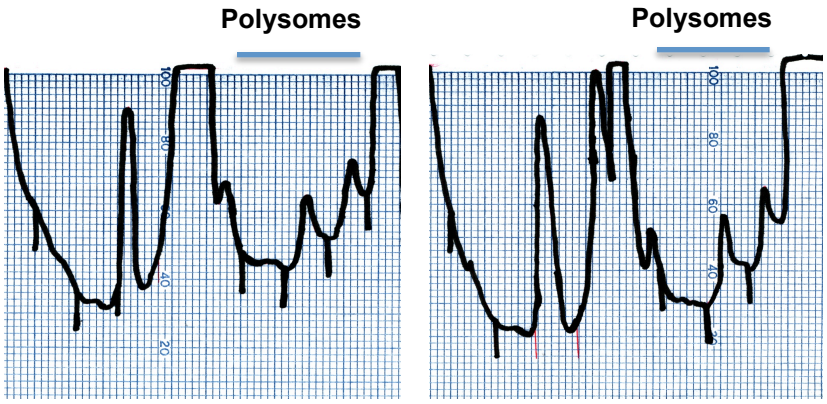

SUDHL6-NS3/4A cells and control cells were lysed in polysome lysis buffer and fractions over sucrose gradients were separated and analyzed by measuring absorbance at 254 nm.

Supplementary Table S1

Table S1 Virological characteristics of patients with chronic HCV infection

Patient	Age	Gender	HCV genotype	Plasma HCV RNA(vge/ml)
1	60	M	1a	6.3×10^{6}
2	63	M	1b	1.1×10^{5}
3	61	M	1a	1.9×10^{6}
4	73	M	1a	7.4×10^{5}
5	62	M	1b	5.3×10^{6}
6	55	M	1a	2×10
7	67	M	1b	1.7×10^{2}
8	50	M	1a	3.6×10^{6}
9	54	M	1a	1.5×10^{6}
10	NA	NA	1a	1.6×10^{7}
11	50	F	2b	6.0×10^{7}
12	51	M	1a	2.9×10^{7}

M, male; F, female; NA, not available; vge, virus genome equivalent;
HCV RNA load measured by real-time RT-PCR using RNA extracted from 250 μl of plasma.